Camphor Sulfonic Acid-hydrochloric Acid Codoped Polyaniline/polyvinyl Alcohol Composite: Synthesis and Characterization

Jorge Enrique Osorio-Fuente,[1]* Carlos Gómez-Yáñez,[1] María de los Ángeles Hernández-Pérez,[1] and Fidel Pérez-Moreno[2]

[1] Departamento de Ingeniería en Metalurgia y Materiales, ESIQIE, Instituto Politécnico Nacional, UPALM, Av. Instituto Politécnico Nacional s/n, CP 07738, México, D. F. josorio@ipn.mx

[2] AACTyM, Universidad Autónoma del Estado de Hidalgo, Carretera Pachuca Tulancingo km 4.5, Mineral de la Reforma, CP 42186, Hidalgo, México.

Abstract. A complementary dopant system formed by hydrochloric and camphor sulfonic (CSA) acids was used in the in-situ synthesis of a polyaniline (PANi)/polyvinyl alcohol (PVA) composite. The conductivity measurements showed that the use of CSA either as single dopant or codopant caused a decrement up to 2 orders of magnitude on the overall conductivity as well as an improvement on thermal stability. The PANi/PVA composites were characterized by spectroscopic and thermal analysis. Conducting emeraldine salt formation was confirmed by UV-VIS and FTIR spectroscopy. Microstructure analysis was performed by SEM imaging.
Key words: Polyaniline, codoping, camphorsulfonic acid, composite.

Resumen. Se utilizó un sistema de dopaje complementario formado por ácido clorhídrico y ácido canforsulfónico (ACS) en la síntesis *in-situ* de un material compuesto polianilina (PANI)/alcohol polivinílico (APV). Las mediciones de conductividad mostraron que el uso de ACS ya sea como dopante o codopante resultó en un decremento en la conductividad total de hasta 2 órdenes de magnitud así como una mejora en la estabilidad térmica. Los compósitos PANi/APV fueron caracterizados mediante análisis térmicos y espectroscópicos. La formación de la sal esmeraldina conductora fue confirmada por espectroscopia UV-Visible e Infrarroja de Transformada de Fourier. El análisis microestructural se llevó a cabo por MEB.
Palabras clave: Polianilina, codopaje, ácido canforsulfónico, material compuesto.

Introduction

Polyaniline (PANi) was the first known electrically conducting polymer. It was synthesized as monomer by Runge [1] and investigated in detail by Fritzsche [2]. Letheby [3] was first in synthesize PANi as the non-conducting, highly-colored polymer known today as semiconducting emeraldine base salt, which was identified in the past as "indigo" and used as dye for clothes. MacDiarmid and Chiang [4] discovered that emeraldine base salt can become conducting after a protonic doping. Furthermore, MacDiarmid and coworkers developed at late 1980s the chemical oxidative polymerization method [5] which involves the use of a strong oxidating agent used as catalyst of the reaction along a suitable protic acid, which acts as dopant. Employing this method it is possible to obtain doped PANi as protonated emeraldine salt, which exhibits conductivity as high as 100 S/cm.

Nowadays PANi has an increasing importance in electronics, having potential applications in several electronic devices such as transistors [6], diodes [7], electromagnetic interference shielding [8], antistatic materials [9], sensing devices [10], and as secondary electrode in all-polymer rechargeable batteries [11]. Also, PANi finds application in the manufacture of anticorrosive coatings [12]. However, the main issue associated with the effective application of PANi is its infusibility and poor solubility in all available solvents [13, 14].

The processability of PANi can be improved substantially by blending it with a commercially available polymer showing both good processability and mechanical properties. Polymer composites containing PANi as conducting filler have received attention because they exhibit a combination of improved processability and good mechanical properties along with good conductivity [15]. Thus, PANi can be blended with, for example, polystyrene [16], poly (methyl methacrylate) [17], methyl cellulose [18], and poly (vinyl alcohol) (PVA) [19]. PVA is a cheap, water soluble polymer with high transparency, very good flexibility and wide commercial availability. In PANi-PVA dispersions, PVA acts as steric stabilizer, preventing PANi from macroscopic precipitation by forming stable dispersions [19], which can be readily post processed as conducting, stand-alone films [20].

In most of the earlier reports [19] dealing with PANi-PVA composite, PVA proved to be a not very good stabilizer for polyanilines. Therefore, composite was synthesized through cosolvation technique [21] using dimethyl acetamide, dimethyl formamide, dimethyl sulphoxide, etc. as solvents. Gospodinova *et al.* [22] were the first to report the synthesis of a stable PANi-PVA dispersion obtained in an aqueous medium.

PANi processing limitations can be also overcome by doping with sulfonic acids molecularly bulky [23], resulting in a PANi which is moderately soluble and further processable both as a aqueous solution or as an organosol. However, the use of these acids as single dopants involves a lower conductivity than PANi doped with inorganic acids due to the lower degree of protonation of the organic acid. Another disadvantage to be taken into account is their high cost. Therefore, on a large-scale production basis, PANi doped with sulfonic acids as single dopants would be commercially unviable. Ruckenstein and Yin

[24, 25] developed a doping technique –termed as codoping or complementary doping– that entails the simultaneous use of the sulfonic acid along a cheap inorganic acid, allowing the synthesis of a soluble PANi showing a conductivity up to 7 S/cm.

In our case, we chemically synthesized PANi doped complementarily by CSA and HCl in the presence of dissolved PVA polymer. We aim to investigate the effect of both CSA and PVA on the conductivity of the resulting composite as well as on its structure and thermal stability. Quite remarkably, despite an evident falling in conductivity due to the inherently insulating PVA matrix and some stiffness of the films, the codoped PANi-PVA composite exhibited a very good processing capability along a moderate conductivity, demonstrating that through appropriate techniques PANi can be converted into a material technologically useful.

Results and Discussion

Fig. 1 shows the UV-VIS absorption spectra of the as-synthesized composites. In the three cases, a broad shoulder around 430-440 nm and a broad band at 840 nm are observed. In absorption spectra of CSA-doped PANi, it has been observed a characteristic broad shoulder that arises from the overlapping between 320 and 420 nm bands [25], ascribed to the elimination of band gap between π and polaron bands [26].

HCl-doped PANi-PVA composite should exhibit a 320 nm absorption band. Its absence suggests that the presence of multi-hydroxyl groups in PVA polymer chains is likely to induce multi-hydrogen bonding with imine/amine groups of PANi [27]. Hydrogen-bonding is known to produce a broad band at 420-440 nm owing to polaron/bipolaron transition [19]. The hypsochromic shift observed in CSA-containing composites has been assigned to a decreasing in the effective π-π^* conjugation [24, 25]. The maximum at about 800 nm can be assigned to a localized polaron [25]. The steadily decreasing tail extending into IR region has been assigned to the free-carriers [19] and is characteristic of conducting polymers with metal-like behavior.

Fig. 2 shows typical infrared spectra of the KBr pellets of PANi/PVA composites as films. The peaks located in 3410-3445 cm^{-1} are related to emeraldine salt (ES) in half-oxidized form [28]. These bands are overlapped with those corresponding to -OH stretching mode of PVA. In the PANi/PVA composite doped with HCl two peaks appear at 3244 cm^{-1} and 3179 cm^{-1} associated with -NH symmetrical stretching mode and the overtone originated by -NH bending in the benzenoid unit. In the composites doped with CSA, these vibrations are overlapped with the peak at 3400 cm^{-1}. The set of vibrations observed in 2915-2925 cm^{-1} as well as those in 2845-2855 cm^{-1} are assigned to stretching mode of -CH aromatic bond. It can be observed bands attributed to C-N stretching mode in the secondary aryl amine in 1615-1620 cm^{-1} for the quinoid unit and in 1575-1610 cm^{-1} for the benzenoid unit. Characteristic vibrations of benzenoid and quinoid units, represented by continous lines at these positions, appear around 1500 and 1600 cm^{-1} [29]. Thus, peaks formerly described have a slightly red shifting, which implies a weakening of the bonds of the polymer chain after doping [30]. Furthermore, intense vibrations at 1380-1385 cm^{-1} are associated with Q = N–B (where Q, quinoid; B, benzenoid) vibration mode. For CSA-doped and HCl + CSA-doped composites there are small vibrations at around 1720 cm^{-1}, related with ketone group of the CSA [23]. The peaks situated in 1430-1470 cm^{-1} are attributed to the stretching mode of the –CH group in the PVA. The peaks in 1260-1300 cm^{-1} range, are assigned to the stretching of the C-N group in the secondary aryl amine of the benzenoid unit. The C-N stretching mode in the secondary aryl amine for quinoid unit is found at 1240 cm^{-1} (HCl-doped PANi/PVA composite). Conversely, for CSA-containing PANi/PVA composites, this vibration appears at 1136 cm^{-1} (CSA+HCl) and 1193 cm^{-1} (CSA). The stretching attributed to in-plane-bending of the –CH group in the benzenoid and quinoid units is located in 1080-1100 cm^{-1} and is overlapped with the C-O
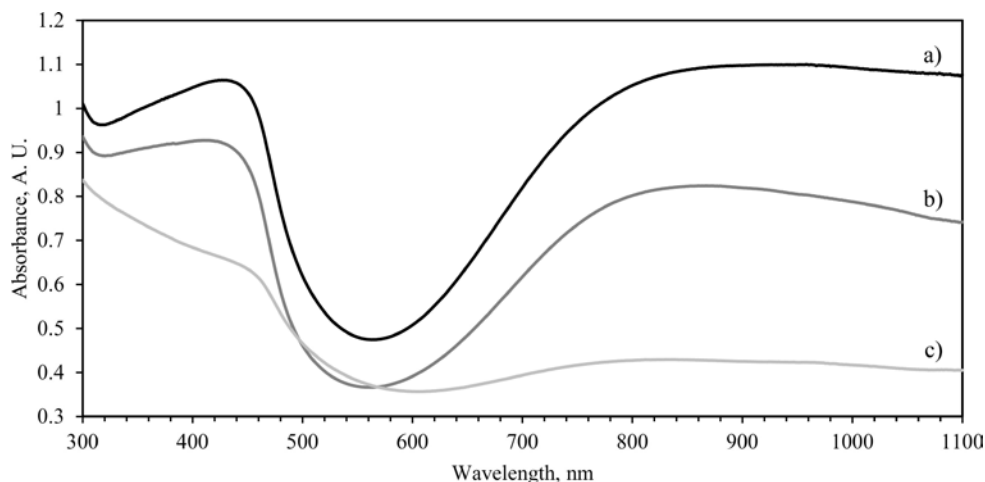

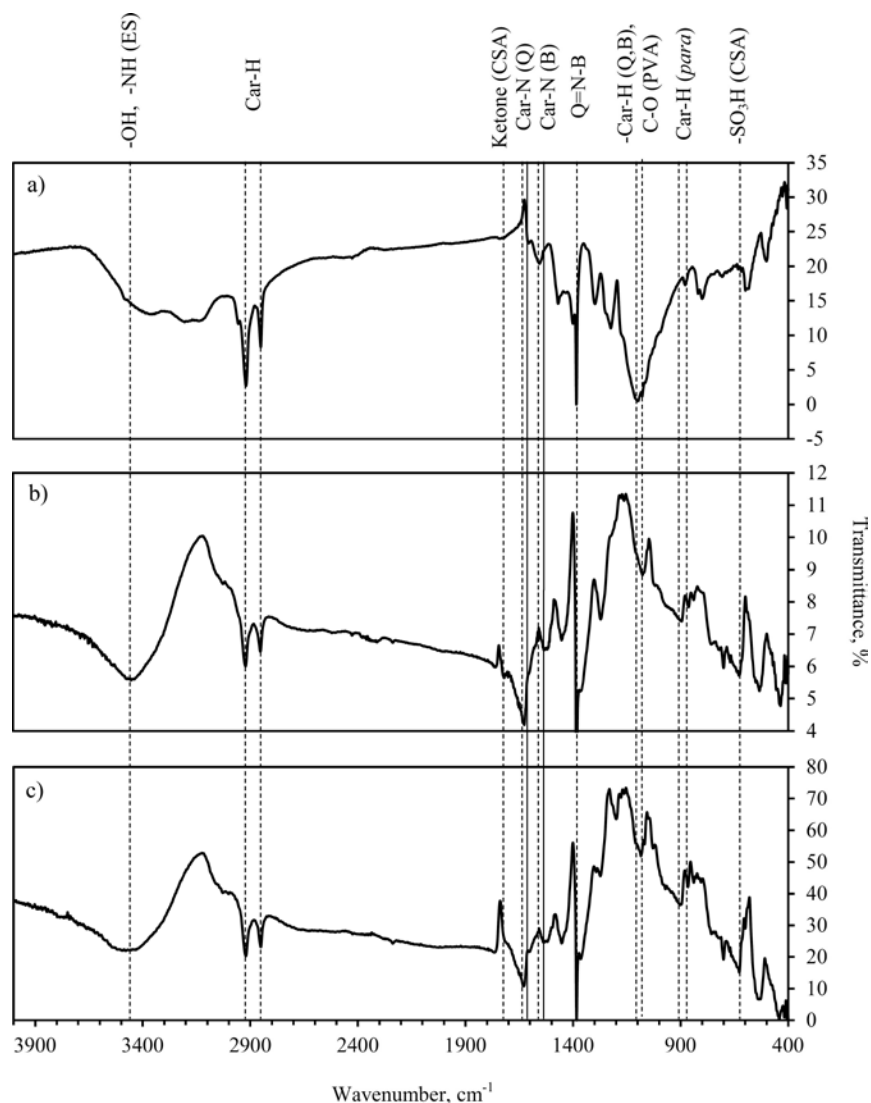**Fig. 1.** UV-Vis spectra of PANI/PVA composites: a) HCl doped; b) HCl+CSA doped; c) CSA doped.

Fig. 2. Infrared spectra of PANi/PVA composites: a) HCl doped; b) HCl+CSA doped; c) CSA doped.

stretching mode in the PVA. This peak is particularly intense in HCl-doped PANi/PVA composite (Figure 2(a)). One possible explanation to the observed differences in intensity between former PANi composite and those doped with CSA assumes that sulfate group $-SO_4^{2-}$, a byproduct of ammonium persulfate decomposition [31], can potentially protonate available imine sites in the polymer main chain. Sulfate ion is known to absorb strongly at around 1090-1100 cm^{-1} [31]. On the other hand, when CSA is used as a dopant, sulfonic acid group from camphorsulfonate ion is more likely to protonate imine sites. Therefore, the intensity of the peak related with SO_4^{2-} decreases accordingly. The peaks appearing in 820-840 cm^{-1} are assigned to C–H out-plane-bending of disubstituted benzene in *para* position [29]. The peaks in 620-625 cm^{-1} for CSA-doped composites confirm the presence of the sulfonic acid group $-SO_3H$ of the organic acid.

Fig. 3 shows the thermograms corresponding to composites under examination. The PANi/PVA composite codoped

with HCl and CSA has a 52% weight loss, the weight losses for PANI/PVA CSA-doped and HCl-doped are 59% and 64%, respectively. There are four stages where changes can be observed in the weight loss rate. The first one comprises the interval located in approximately between 60 °C and 150 °C. The second one takes place from 150 °C and up to 220 °C. In the third stage occurs a remarkable increasing in the weight loss, reaching its highest point near to 340 °C for the composites doped with CSA and near to 360 °C for the composite doped with HCl, presenting this material the highest weight loss.

In the fourth stage it can be observed that there is a small weight loss. The mechanism of thermal decomposition is, according to [20, 32], as follows: the first stage corresponds to removal of moisture and water from PVA matrix. The second stage corresponds to nearly two simultaneous events: the crosslinking of PANi and removal of the molecules of dopant. In the third stage take place crosslinking reactions in the PVA matrix, which produce polyenic structures and volatile prod-

ucts. Finally the fourth stage is attributed to total decomposition of both the host matrix and the semiconducting polymer. Consequently, for practical purposes the working temperature of PANi composites would not exceed 130 °C.

Differential thermal analysis (DTA) curves can be seen in Fig. 4. Concerning to PANi/PVA composites doped with HCl and CSA as single dopants, it can be noted a wide endotherm event ranging from 90 to 190 °C. This endotherm appears also in the codoped composite in the 140-190 °C range, but it is narrower. Glass transition temperature (T_g) of the composites is situated in the range from 140 to 160 °C. The endotherms that appear in the range from 190 to 320 °C correspond to crosslinking reaction of PVA, removal of dopants (chloride, camphorsulfonate) and the production of polyenic structures and volatile products [33]. Finally, the process of total degradation of the polymer takes place in the range of temperatures between 330 to 370 °C, reaching its highest point in 380 °C. From this point on, the values of heat flow are constant. The final by-products of the thermal degradation are constituted mainly of carbon and high molecular weight hydrocarbons [34].

The Table 1 summarizes T_g values of PANi/PVA composites.

For PANi doped with HCl and CSA as single dopants, a T_g of 87 °C and 150 °C has been reported [35,36], respectively. T_g of PVA is around 85 °C [37]. The increasing of T_g observed in PANi/PVA composites with reference to pristine materials could be ascribed to the strong interaction between hydroxyl groups of PVA and hydrogen atoms of amine/imine groups, which hinders molecular motion of local segments in conducting polymer main chain. Likewise, CSA is expected to experiment a stronger interaction with hydroxyl groups of PVA than HCl, therefore leading to a rising on the T_g. Indeed, CSA doped PANi/PVA composites exhibit an increment on T_g. Actually, complementary doping increases remarkably glass transition temperature of the conducting composite.

SEM micrographs of the composites can be observed in Fig. 5. The morphology of the composites consists essentially of a heterogeneous microstructure formed by spheroidal granules in the range of microns alternating with flake-like laminar layers of PVA. Granules are organized into inhomogeneously
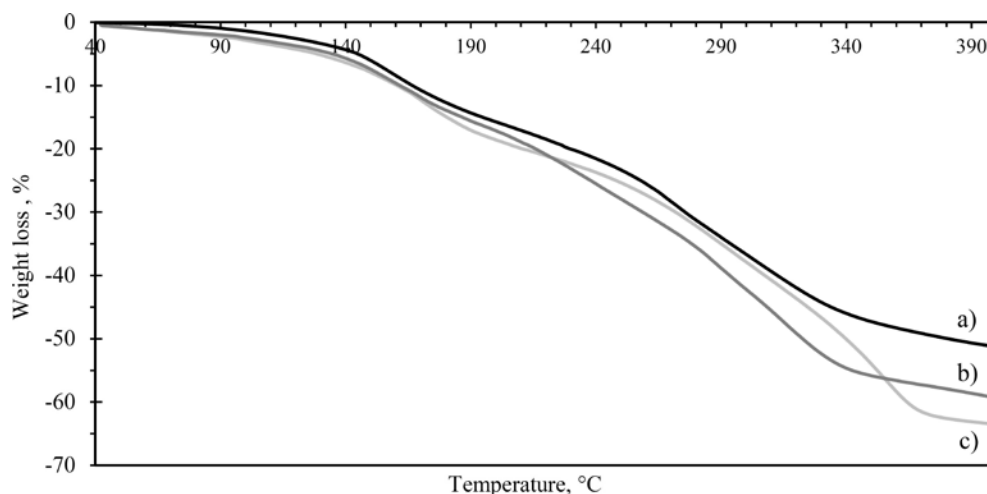

Fig. 3. TGA thermograms, a) PANi/PVA HCl+CSA codoped, b) PANi/PVA HCl doped and c) PANi/PVA CSA doped.
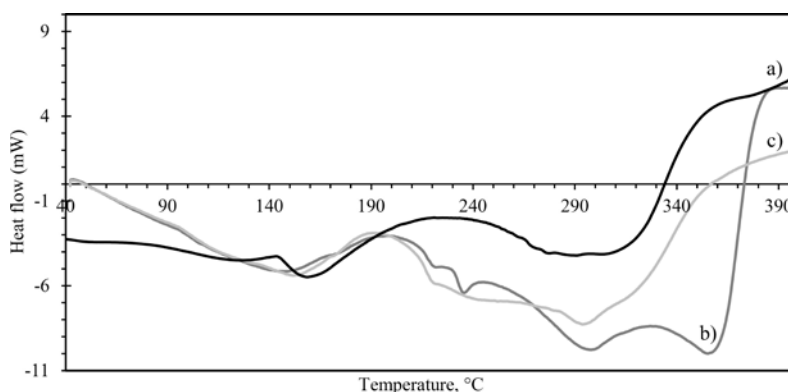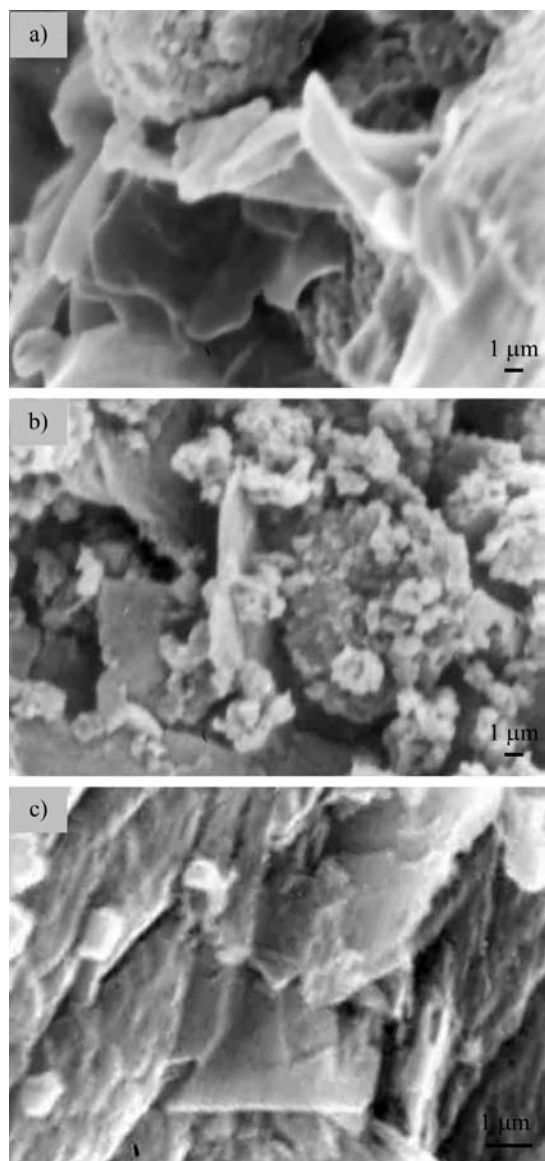

Fig. 4. DTA thermograms, a) PANi/PVA HCl+CSA codoped, b) PANi/PVA HCl doped and c) PANi/PVA CSA doped.

Table 1. Glass transition temperature of the as-synthesized PANI/PVA composites.

Composite	T_g (°C)
PANi/PVA, HCl doped	145
PANi/PVA, CSA doped	150
PANi/PVA, HCl+CSA doped	160

Table 2. Conductivity measurements of the PANI/PVA composite films.

Composite	Conductivity (S/cm)
PANi/PVA, HCl doped	1.3×10^{-3}
PANi/PVA, CSA doped	1.8×10^{-5}
PANi/PVA, HCl+CSA doped	5.0×10^{-5}

Fig. 5. SEM micrographs of PANi/PVA composites: a) HCl-doped, b) CSA-doped, c) HCl+CSA codoped.

distributed clusters. Granular aggregates are a characteristic morphological feature [38] of PANi with a heterogeneous nucleation mechanism [39].

Results of conductivity measurements can be seen in Table 2. As expected, composites show reduced conductivity due to intrinsic insulating nature of PVA host matrix, however, it can be noted a difference up to 2 orders of magnitude between

PANi/PVA doped with HCl and the CSA-doped PANi/PVA composites' conductivity. CSA induces geometric deformation resulting in an increasing on torsion angle between adjacent fenile rings due to camphorsulfonate ion bulky molecule [40]. Further, CSA also gives place to an steric hindrance by electrostatic repulsion between doping ion and hydrogen of the imine sites [41]. Therefore, effective conjugation length decreases affecting conductivity negatively [25]. The slight increase observed in conductivity of CSA + HCl codoped PANi/PVA composite is attributed to PANi moieties doped by Cl⁻ chloride ion, since HCl promotes a conducting structure in the polymer [25].

Conclusions

Moderately conducting PANi/PVA composites doped with HCl, CSA and HCl + CSA could be synthesized. PVA gives place to the formation of stable and easily processable dispersions of PANi, which can be casted into films. UV-VIS and IR studies confirmed that PANi in the composites is in half-oxidized form, protonated emeraldine salt.

The use of CSA either as single or complementary dopant resulted in a decrement in the conductivity, however CSA improves the thermal stability of the conducting composite. Thus, in spite of modest values of conductivity, the codoped composite could be used as a promissory material where low conductivities are not a decisive factor, for example in the manufacture of antistatic shielding.

Experimental

Reagents

PVA was purchased from DuPont and the average molecular weight was Mw = 100000. Aniline hydrochloride (Fluka), hydrochloric acid (Fermont), camphorsulfonic acid (Fluka) and ammonium persulfate (Sigma-Aldrich) were analytical grade and used as received. Distilled water was used in all experiments.

Synthesis

The synthesis of the codoped PANi/PVA composite was carried out by dissolving 20 mmol (2.59 g) of aniline hydrochloride in 50 mL of a 10 wt% aqueous solution of PVA. The polymeriza-

tion was initiated at room temperature by drop-wise addition under constant stirring of 50 mL of an aqueous solution containing 15 mL of CSA [1 M], 35 mL of HCl [1 M] and 25 mmol (5.71 g) of ammonium persulfate (APS). The volumetric HCl: CSA ratio and molar aniline:oxidant ratio were kept in 70:30 and 1:1.25, respectively. After complete addition of the former solution, the reaction mixture was stirred for 3 h. The film of codoped PANI/PVA composite was obtained by pouring the black-green dispersion on the bottom of a 10 cm in diameter Petri dish previously covered with a plastic paraffin film piece. The dispersion was then dried for 6 h at 60 °C. Once finished the drying process, the PANi/PVA composite film sample was separated from the substrate, washed with distilled water and acetone, wrapped with absorbing tissue and stored in a self-sealable bag. In the cases of conducting composites doped only with either HCl or CSA, the aqueous solution consisted of 50 mL of the dopant (HCl [1 M] or CSA [1 M]) and 25 mmol (2.59 g) of APS, the same procedure above described was followed for the synthesis of dispersion and processing of the film.

Characterization

Electrical conductivity

From each film sample a 1 cm × 1 cm square section was cut. The samples were masked and coated with a Au-Pd coating by using a Denton Vacuum Desk V sputtering system, in order to obtain a centered contact of 5 mm in diameter on both sides. Copper leads were attached to each Au-Pd contact by using silver paste. Resistance measurements were done using a common digital multimeter. Conductivity was determined by standard Van der Pauw two-probe method.

UV-VIS spectroscopy

From each PANi/PVA dispersion a sample volume of 0.1 mL was taken in order to be dissolved in 20 mL of distilled water. Absorbance spectra from 300 to 1100 nm were recorded on a Perkin Elmer Lambda 35 spectrometer using a set of paired cells of 1 cm optical path length and distilled water as reference solvent.

FTIR spectroscopy

Infrared spectra were taken on a FT-IR Perkin Elmer System 2000 spectrometer between 400 and 4000 cm^{-1} region and were corrected for CO_2 and H_2O content in the optical path. The samples were prepared in the pellet form using spectroscopic grade KBr powder.

TGA and DTA measurements

Thermogravimetric analyses (TGA and DTA) were carried in a Setaram SetSys Evolution TGA-DTA instrument at a heating rate of 10 °C/min up to 400 °C under argon flow.

SEM imaging

15 mL of each PANi/PVA dispersion were filtered, washed with distilled water and acetone, and then dried in an oven at 60 °C overnight. The black-green powder was grounded and a small quantity was put on a specimen holder previously coated with graphite conducting tape. The morphology of the powders was observed using a JEOL JSM 6300 microscope without conductive coating on samples at a 10 kV acceleration voltage.

Acknowledgements

References

1. Runge, F. F. *Poggendorfs Ann. Physik u. Chemie* **1834,** *31,* 513-524.
2. Fritzsche J. *J. Prakt. Chem.* **1840**, *20*, 454.
3. Letheby, H. *J. Chem. Soc.* **1862**, *15*, 161-163.
4. MacDiarmid, A. G.; Chiang, J. C. *Synth. Met.* **1986**, *13*, 193-205.
5. MacDiarmid, A. G.; Chiang, J. C.; Richter, A. F.; Epstein, A. J. *Synth. Met.* **1987**, *18*, 285-290.
6. Pinto, N. J.; Johnson, A. T.; MacDiarmid, A. G.; Mueller, C. H.; Theofylaktos, N.; Robinson, D. C.; Miranda, F. A. *Appl. Phys. Lett.* **2003**, *83*, 4244-4246.
7. Zhao, C.; Xing, S.; Yu, Y.; Zhang, W.; Wang, W. *Microelectron. J.* **2007**, *38*, 316-320.
8. Bhadra S.; Singha N. K.; Khastgir D. *Polym. Eng. Sci.* **2008***, 48*, 995-1006.
9. Ohtani A.; Abe M.; Ezoe M.; Doi T.; Miyata T.; Miyke A. *Synth. Met.* **1993**, *57*, 3696-3701.
10. Bhadra, S.; Khastgir, D.; Singha, N. K.; Lee, J. H. *Prog. Polym. Sci.* **2009**, *34*, 783-810.
11. Qiao, Y.; Li C. M.; Bao S. J.; Bao Q. L. *J. Power Sources* **2007**, *170*, 79-84.
12. Armelin, E.; Pla, R.; Liesa, F.; Ramis, X.; Iribarren, J. I.; Alemán, C. *Corr. Sci.* **2008**, *50*, 721-728.
13. Cho, M. S.; Park, S. Y.; Hwang, J. Y.; Choi, H. J. *Mater. Sci. Eng. C* **2004**, *24*, 15-18.
14. Rao, P. S.; Subrahmanya, S.; Sathyanarayana, D. N. *Synth. Met.* **2003**, *139*, 397-404.
15. Bhadra, S.; Singha, N. K.; Khastgir, D. *J. Appl. Polym. Sci.* 2008, *107*, 2486-2493.
16. Ruckenstein. E.; Yang, S. *Synth. Met.* 1993, *53*, 283-292.
17. Dhawan, S. K.; Singh, N.; Rodrigues, D. *Sci. Tech. Adv. Mater.* 2003, *4*, 105-113.
18. Chattopadhyay D.; Mandal, B. M. *Langmuir* 1996, *12*, 1585-1588.
19. Gangopadhyay, R.; De, A.; Ghosh, G. *Synth. Met.* **2001,** *123*, 21-31.
20. Gangopadhyay, R.; De, A. *Synth. Met.* **2002**, *132*, 21-28.
21. Ogura, K.; Saino, T.; Nakayama, M.; Shiiji, H. *J. Mater. Chem.* **1997**, *7*, 2363-2366.
22. Gospodinova, N; Mokreva, P.; Terlemezyan, L. *J. Chem. Soc., Chem. Comm.* **1992**, *13*, 923-924.
23. Jaymand, M. *Prog. Polym. Sci.* **2013**, *38*, 1287-1306.
24. Yin, W.; Ruckenstein, E. *Synth. Met.* **2000**, *108*, 39-46.
25. Yin, W.; Ruckenstein, E. *J. Appl. Polym. Sci.* **2001**, *79*, 80-85.

26. Xia, Y.; Wiesinger, J. M.; MacDiarmid, A. G. *Chem. Mater.* **1995**, *7*, 443-445.

27. Mohamoud M. A, *J. Solid State Electrochem.* **2013**, DOI 10.1007/s10008-013-2174-4

28. Raupp-Cardoso, M. J.; Santos-Lima, M. F.; Lenz, D. M. *Mat. Res.* **2007**, *10*, 425-429.

29. Wang, Y.; Rubner, M. F. *Synth. Met.* **1992**, *47*, 255-266.

30. Kuo, C. –T.; Chen, C. –H. *Synth. Met.* **1999**, *99*, 163-167.

31. Trchová, M.; Stejskal, J.; Prokeŝ, J. *Synth. Met.* **1999**, *101*, 840-841.

32. Hino, T.; Namiki, T.; Kuramoto, N. *Synth. Met.* **2006**, *156*, 1327-1332.

33. Stejskal, J.; Omastová, M.; Fedorova, S.; Prokeŝ, J.; Trchová, M. *Polymer* **2003**, *44*, 1353-1358.

34. Chen, T.; Dong, C.; Li, X.; Gao, J. *Polym. Deg. and Stab.* **2009**, *94*, 1788-1794.

35. Li, J.; Tang, X.; Li, H.; Yan, Y.; Zhang, Q. *Synth. Met.* **2010**, *160*, 1153-1158.

36. Abell, L.; Pomfret, S. J.; Adams, P. N.; Monkman, A. P. *Synth. Met.* **1997**, *84*, 127-128.

37. Vinyl alcohol polymers in: *Encyclopedia of Polymer Science and Technology*, Vol. 8, John Wiley and Sons, Ed., Hoboken, N. J., **2011**, 401.

38. Saravanan, S.; Joseph Mathai, C.; Anantharaman, M. R.; Venkatachalam, S.; Prabhakaran*,* P. V. *J. Phys. and Chem. Sol.* **2006**, *67*, 1496-1501.

39. Xing, S.; Zheng, H.; Zhao, G. *Synth. Met.* **2008**, *158*, 59-63.

40. Yue, J.; Wang, Z. H.; Cromack, K. R.; Epstein, A. J.; MacDiarmid, A. G. *J. Am. Chem. Soc.* **1991**, *113*, 2665-2671.

41. Sinha, S.; Bhadra, S.; Khastgir, D. *J. Appl. Polym. Sci.* **2009**, *112*, 3135-3140.